iScience

CellPress
OPEN ACCESS

Perspective

Infinite possibilities of ultrathin III-V semiconductors: Starting from synthesis

Fangyun Lu,[1,2] Huiliu Wang,[1,2] Mengqi Zeng,[1,*] and Lei Fu[1,*]

SUMMARY

Ultrathin III-V semiconductors have been receiving tremendous research interest over the past few years. Owing to their exotic structures, excellent physical and chemical properties, ultrathin III-V semiconductors are widely applied in the field of electronics, optoelectronics, and solar energy. However, the strong chemical bonds in layers are the bottleneck of the two-dimensionalization preparation process, which hinders the further development of ultrathin III-V semiconductors. Some effective methods to synthesize ultrathin III-V semiconductors have been reported recently. In this perspective, we briefly introduce the structures and properties of ultrathin III-V semiconductors firstly. Then, we comprehensively summarize the synthetic strategies of ultrathin III-V semiconductors, mainly focusing on space confinement, atomic substitution, adhesion energy regulation, and epitaxial growth. Finally, we summarize the current challenges and propose the development directions of ultrathin III-V semiconductors in the future.

INTRODUCTION

The successful preparation of atomic thin graphene and exploration of its intrinsic properties extensively boost the research of two-dimensional (2D) materials (Novoselov et al., 2004). The large surface area, mechanical, optical, and electronic properties make the 2D materials, such as graphene, MoS_2, BN, C_3N_4 and so forth, promising in the field of photocatalysis, electrocatalysis, single-atom catalysis, energy storage, sensors, and optoelectronics (Feng et al., 2011; Liang et al., 2017; Mishra et al., 2019; Tang and Jiang, 2016; Van Dao et al., 2021; Wang et al., 2017b; Zhang, 2015; Zhi et al., 2009; Zhu et al., 2011). III-V semiconductors with exotic structures, direct band gap and high carrier mobility have great potential in manufacturing solar cells, lasers, photodetectors, light-emitting diodes, and other devices, which have attracted tremendous attention in 2D materials (Chen et al., 2016; Cipriano et al., 2020; del Alamo, 2011; Kobayashi et al., 2012; Wallentin et al., 2013; Zhang et al., 2019). When III-V semiconductors come to two dimensions, unique properties emerge, including 2D electron and hole gas, blue-shifted band gap, and nonlinear optics, bringing them a broader application space (Al Balushi et al., 2016; Ambacher et al., 1999; Chaudhuri et al., 2019; Sanders et al., 2017). However, III-V semiconductors are deemed as a class of non-layered compounds, which have obvious differences in structures from 2D layered materials (Dou et al., 2017). For 2D layered materials, they are bonded by strong chemical bondings in plane, while in the three-dimensional direction each layer is stacked by weak van der Waals interactions. This structural feature makes 2D layered materials easy to be obtained by exfoliation. The 2D non-layered compounds, however, are kept together by strong chemical bondings both in plane and out of plane, which prevent their exfoliation and 2D anisotropic growth (Dou et al., 2017; Wang et al., 2017a). Therefore, the controllable growth of ultrathin non-layered III-V semiconductors is still challenging.

Here, we are committed to summarizing the current synthesis strategies of ultrathin III-V semiconductors, including space confinement, atomic substitution, adhesion energy regulation, and epitaxial growth. The structures and properties of ultrathin III-V semiconductors are also introduced. We hope that the perspective can bring new insights into the synthesis of ultrathin III-V semiconductors and provide a platform for the exploration of properties and applications in the foreseeable future.

STRUCTURES OF ULTRATHIN III-V SEMICONDUCTORS

Considering the many advantages of 2D geometry of materials, exploring ultrathin III-V semiconductors system is necessary. III-V semiconductors usually possess two relatively stable structures. The nitrides

[1]College of Chemistry and Molecular Sciences, Wuhan University, Wuhan 430072, China

[2]These authors contributed equally

*Correspondence: leifu@whu.edu.cn (L.F.), zengmq_lan@whu.edu.cn (M.Z.)

https://doi.org/10.1016/j.isci.2022.103835

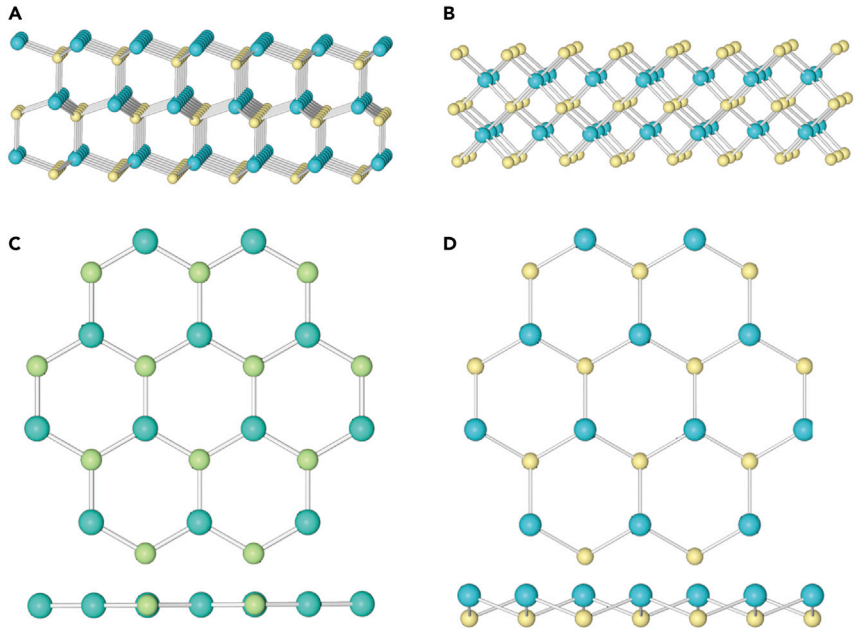

Figure 1. Structures of III-V semiconductors

(A) Wurtzite structure of III-V semiconductors.

(B) Zinc blende structure of III-V semiconductors.

(C) Planar structure of III-V semiconductors.

(D) Buckled structure of III-V semiconductors.

mainly crystallize in the wurtzite crystal structure with $P6_3mc$ space group, and the other materials (AlP, AlSb, GaP, GaSb, InP, InSb) exist in the zinc blende structure with the F43m space group (Figures 1A and 1B) (Kuech, 2016). Unlike the layered materials bonded by weak van der Waals bonds in interlayers, the covalent bonds in layers of these structures lead to the non-layered nature of III-V semiconductors (Kolobov et al., 2016). Large lattice structural distortion of non-layered materials appears in the 2D limit, leading to abundant unsaturated dangling bonds covered on the surface of ultrathin III-V semiconductors, which results in high chemical activity on the surface, making it easier to adsorb gas molecules and promising in catalysis and sensing (Wang et al., 2017a).

In addition, Zhuang et al. predicted that monolayer nitrides and AlP tend to form planar structure, while others such as AlSb, GaP, GaSb, InP, and InSb are more likely to form buckled structure (Figures 1C and 1D). The emerging trend of these structures can be explained from two aspects: the electrostatic potential energy and the bond energy of sp^2 and sp^3 hybridization of group III and V ions. On the one hand, the layered hexagonal materials with alternating buckled structure lead to the dipole moment passing through the layer, the electrostatic energy of which is proportional to Q^2/a^2 (Q: ionic charge, a: lattice parameter). The large electronegativity difference of the constituent species in nitrides and AlP leads to a large ionic charge. At the same time, the small lattice parameters lead to large electrostatic energy. Therefore, the buckled structure in nitrides and AlP is unfavorable. On the other hand, the conclusion about structure trend cannot be explained by electrostatic interaction alone. The sp^2 and sp^3 hybridization of ions in III-V semiconductors also needs to be considered. The III-group elements can form a planar triangular structure with D_{3h} symmetry by sp^2 hybridization, whereas the V-group elements tend to form pyramidal trigonal configuration by sp^3 hybridization. As far as nitrogen atom, if the lone pair occupies a p orbital, it participates in the aromatic bond by forming π bond, and the triangular plane configuration can be formed. However, phosphides and heavier group V elements compounds are more advantageous in sp^3 hybridization so that they tend to form a pyramidal trigonal configuration with C_{3v} symmetry. Combining the two results above, the conclusion that the planar hexagonal configuration only belongs to nitrides and AlP can be drawn (Şahin et al., 2009; Zhuang et al., 2013).

PROPERTIES OF ULTRATHIN III-V SEMICONDUCTORS

Piezoelectric

The anisotropy of 2D crystal structures is more significant than that of bulk materials, which is caused by the reduction of dimension. Particularly, piezoelectricity will appear in 2D structures because inversion symmetry is eliminated. Therefore, the ultrathin III-V semiconductors with hexagonal planar and buckled structure are likely to exhibit piezoelectric properties because of breaking the inversion symmetry. Blonsky et al. predicted that the metal dichalcogenides, oxides, and III-V semiconductors with planar structure exhibit an in-plane piezoelectric coefficient. InN possesses a prominent value of 5.50 pm/V among them. In particular, the ultrathin III-V semiconductors with the buckled structure such as GaSb, InP, and InSb exhibited out-of-plane piezoelectric coefficients ranging from 0.02 to 0.6 pm/V. The existence of piezoelectricity in ultrathin III-V semiconductors enables their application in energy conversion. The possibilities of applying ultrathin III-V semiconductors in the nanorobots, piezoelectric electronics, and nanoelectromechanical systems, such as actuators, sensors, and energy collectors may be realized on the premise of this property (Blonsky et al., 2015).

Optical

The different optical properties of III-V semiconductors will appear in the 2D limit. It is reported that the light emission of ultrathin III-V semiconductors will be blue shifted. Compared with bulk GaN, monolayer GaN emits in the deep UV range, which is promising in sterilization and water purification. Similarly, the 2D InN optical absorption peaks have a blue-shift compared to bulk InN, which brings it new potential in near-infrared regime (Liang et al., 2017).

Besides, the strongly polarized light emission and excellent nonlinear optical properties will occur in the 2D limit of III-V semiconductors (Sanders et al., 2017). Chen et al. successfully tested the second harmonic generation (SHG) of 2D InP and InSb after preparing a series of ultrathin III-V semiconductors. Taking InP as an example, the polarization-resolved SHG suggested a 6-fold anisotropic behavior of 2D InP single crystal. Moreover, SHG can be employed to study the crystal quality and stacking modes (Chen et al., 2020; Kumar et al., 2013; Li et al., 2018).

Electronic

Taking advantage of the atomic-thin thickness, the generation of quantum confinement effect in ultrathin III-V semiconductors leads to a wider band gap, such as GaN, AlN, InN, InP, and InSb (Brus, 1984). It has been reported that the band gap of 2D AlN is about 9.2 eV while the band gap of its bulk counterparts is only 6.2 eV, which endows it with the ability to be used in UV photoelectric devices (Wang et al., 2019a, 2019b). The band gap of 2D GaN is wider than that of bulk counterparts which have also been discovered in the experiment (Al Balushi et al., 2016). In addition, the electronic property of ultrathin III-V semiconductors can be regulated. It's predicted that the band gap of 2D GaN will be changed by tuning the ratio of Ga and N. Decreasing the ratio of Ga vacancies could increase the band gap of 2D GaN, which means the band gap can be artificially adjusted by introducing vacancies into 2D GaN (Wang et al., 2021).

Thermoelectric

The thermoelectric property of ultrathin III-V semiconductors has also been studied to explore the applications in thermoelectric devices. First of all, the abnormal thermal conductivity of III-V semiconductors in the 2D limit has been discovered. Although the monolayer GaN possesses a planar structure similar to graphene, its thermal conductivity is much lower than that of graphene. Moreover, its thermal conductivity is more than one order of magnitude lower than that of bulk GaN and even lower than that of silicene with a distorted structure. Qin et al. found that the large difference in atomic radius and mass between Ga and N atoms leads to the lowered symmetry in 2D GaN, which broke the phonon-phonon scattering selection rule and caused abnormal thermal conductivity. At the same time, the electronic structure analysis indicated that the Ga-d orbital in monolayer GaN mediates the particular sp orbital hybridization, the strongly Ga-N bond polarization, localized charge density, and its non-uniform distribution, which lead to the inherent low thermal conductivity. This abnormal phenomenon endows it broad application prospects in energy conversion (Qin et al., 2017).

Besides, considering that 2D InN has high electron mobility, electrical conductivity, Seebeck coefficient, and low thermal conductivity, it's a promising candidate for non-toxic, stable thermoelectric applications (Yeganeh et al., 2020).

Catalytic

The abundant unsaturated dangling bonds on the surface of ultrathin III-V semiconductors can serve as the active sites for adsorbing gas, which makes ultrathin III-V semiconductors the excellent candidate in catalysis and sensing, such as GaN and AlN (Chen et al., 2019; Wang et al., 2017a). Taking AlN as an example, the Al and N atoms are 3-fold-coordinated with dangling bonds covered on the 2D AlN surface, which is different from its bulk counterparts with four coordination and enables the gas adsorption. Besides, the Al-N bond is polarized owing to the charge transfer from Al to N, which also leads to gas molecules adsorbed on the AlN sheet directly through electrostatic and polarization interactions (Wang et al., 2018b).

In addition, the hybrid of ultrathin III-V semiconductors with other compounds can further broaden the applications of them in catalysis (Cipriano et al., 2021; Hu et al., 2014; Zeng et al., 2015). It is predicted that 2D InP/TiO_2 heterojunction will show a high photocatalytic performance. Firstly, the strong chemical bonds in the interface of them enable the formation of 2D InP/TiO_2 heterojunction, whose band edge possesses the type-II alignment. The photogenerated carriers will be generated in 2D InP owing to their excellent light absorption ability. Then, the photogenerated electrons migrate from InP to TiO_2 because the band edges energy of TiO_2 is lower. This transfer process achieves the effective electron-hole separation and guarantees high photocatalysis efficiency.

Others

Some of the low-dimensional III-V semiconductors have been deemed as a promising platform for topological quantum computation. For instance, 2D InSb has great potential in this certain field for the low effective mass, strong spin-orbit interaction, high carrier mobility, and narrow band gap (Zhi et al., 2019). The high carrier mobility of 2D InSb has been demonstrated by applying its nanostructure on spin Hall devices. The mobility was found as high as 20,000 $cm^2 V^{-1} s^{-1}$, which is remarkable among the common 2D materials system (Liu et al., 2014; Long et al., 2009; Schmidt et al., 2014). It strongly suggested that the system is a feasible nanoscale 2D platform for quantum devices in the future (Gazibegovic et al., 2019).

More than that, extrinsic properties of ultrathin III-V semiconductors will appear by introducing vacancies and chemical doping (Wang et al, 2021; Zhao et al., 2016). Taking GaN as an example, theoretical prediction shows that the Ga vacancies in 2D GaN lead to nonzero magnetic moments. A magnetic tunnel junction can be designed by GaN containing Ga vacancies instead of the traditional ferromagnetic metal as the ferromagnetic layer.

Although theoretical studies indicated that ultrathin III-V semiconductors possess excellent properties and bright application prospects, few of them have been proved in experiments. The main obstacle hindering the application progress of ultrathin III-V semiconductors is preparation. Therefore, a summary of effective synthesis strategies is necessary for the development of ultrathin III-V semiconductors.

SYNTHESIS STRATEGY

Although the ultrathin III-V semiconductors possess several excellent properties, the synthesis of ultrathin III-V semiconductors remains challenging. Owing to the existence of chemical bondings in 3D direction, the methods employed in 2D layered materials are insufficient to realize the synthesis of ultrathin III-V semiconductors. To achieve the growth of ultrathin III-V semiconductors, various strategies have been developed. Here, we are committed to summarizing some effective growth strategies for synthesizing ultrathin III-V semiconductors in recent years, mainly including space confinement, atomic substitution, adhesion energy regulation, and epitaxial growth strategy (Figure 2). These strategies may spark new ideas for the controllable growth of ultrathin III-V semiconductors.

Space confinement

Space confinement strategy can limit the vertical growth of 2D non-layered materials to satisfy the requirement of the controllable thickness (Wang et al., 2018a; Zhou et al., 2018). Confined space constructed by overlayer and substrate can physically constrain the vertical growth of ultrathin III-V semiconductors. The overlayer can also stabilize the formed structure. In 2016, 2D GaN was successfully fabricated in the confined space between graphene and 6H-SiC (Al Balushi et al., 2016). The graphene was obtained from the sublimation of silicon from the surface of SiC (0001). Meanwhile, to promote Frank-van der Merwe growth mode of GaN, an interface with reduced surface energy was constructed via hydrogenation which

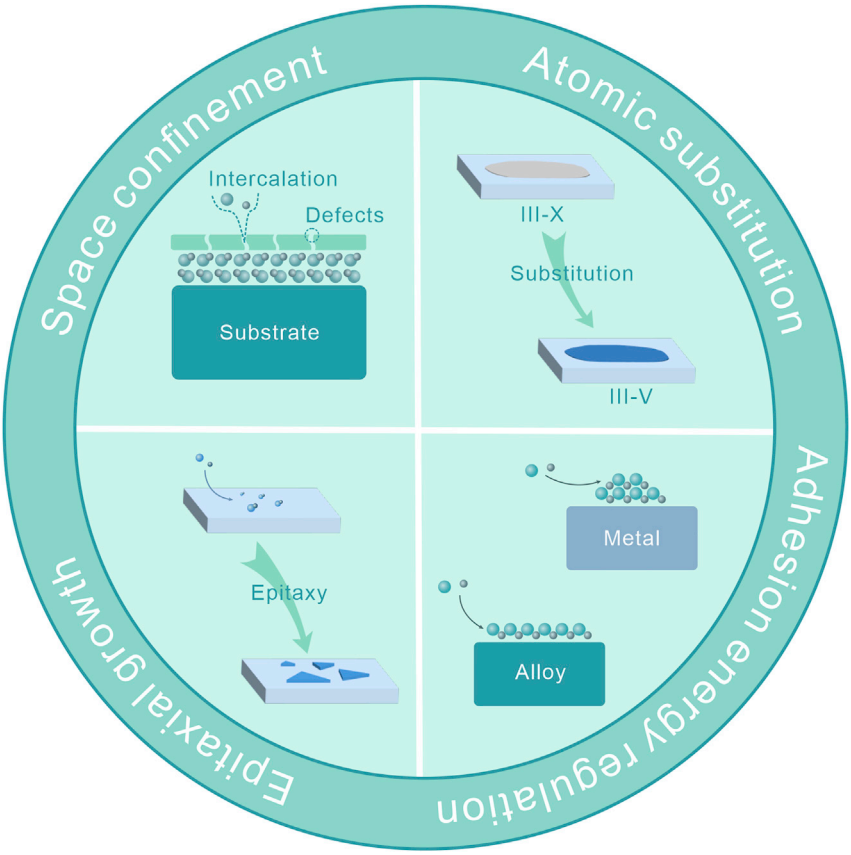

Figure 2. Schematic diagram of different synthesis strategies

passivated dangling bonds between graphene and SiC. In addition, defects in graphene facilitated gallium intercalation. Finally, the intercalated gallium was transformed into 2D GaN by the ammonolysis process. Graphene provided an energetically stable interface for the growth of 2D GaN. The trend of forming 3D GaN was more obvious without the graphene layer.

Similarly, Wang et al. reported the confined growth of 2D AlN layers between graphene and Si substrate by the metal organic chemical vapor deposition (Wang et al., 2019b). To construct a limited region for the epitaxial growth of 2D AlN, graphene was transferred to Si (111) surface. A hydrogenation process was subsequently used to generate defects in graphene (Riedl et al., 2009), thus enabling the intercalation of Al and N atoms decomposed from precursors (Figure 3A). Thereafter, Al and N atoms reacted in the interlayer between graphene and Si and 2D AlN was successfully fabricated (Figures 3B and 3C). 2D AlN was located at the graphene/Si (0001) interface confirmed by the electron energy loss spectroscopy (Figure 3D). Similar to the growth process of 2D GaN and 2D AlN, 2D InN was also fabricated by the same space confinement growth strategy in 2021 (Pécz et al., 2021). In general, in the growth process of the III-V semiconductors, limited space between graphene and substrate is essential and the graphene layer plays an important role in stabilizing the structure.

In addition, ultrathin III-V semiconductors can be prepared by liquid metal-assisted confined growth strategy. The 2D single-crystalline InP was successfully fabricated by low-pressure chemical vapor deposition (CVD) (Chen et al., 2016). Liquid metal In was lithographically patterned onto a substrate with a MoO_x nucleation layer, then In was confined by evaporated SiO_x as illustrated in Figure 3E. Afterward, in the atmosphere of phosphine (PH_3) and H_2, phosphorus reacted with In and formed InP nucleus. A phosphorus depletion zone formed around the nucleus zone, pre-designing In in the confined substrate made the In template fully occupied by phosphorous depletion zone from the first nucleus, thus promoting its single crystalline growth.

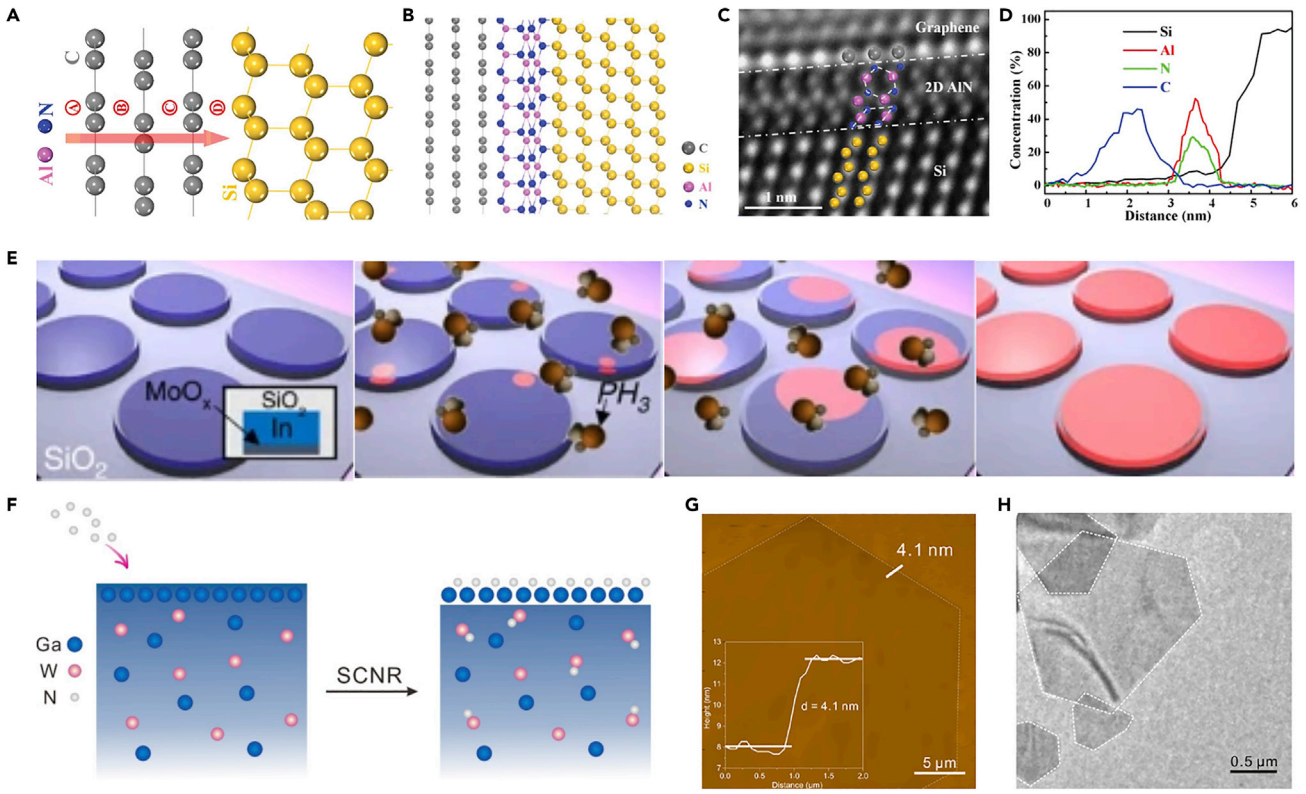

Figure 3. Space confinement growth of III-V semiconductors

(A) Schematic diagram of the intercalation process of Al and N atoms.

(B) Schematic diagram of 2D AlN sandwiched between graphene and Si.

(C) Cross-sectional TEM image of AlN layers at high magnification.

(D) Electron energy loss spectroscopy for graphene/2D AlN/Si heterostructure. Images A-D reproduced with permission from (Wang et al., 2019b). Copyright 2019 John Wiley and Sons.

(E) Schematic diagram of the growth progress of InP crystal. Image reproduced with permission from (Chen et al., 2016). Copyright 2016 Springer Nature.

(F) Growth mechanism of 2D GaN.

(G) AFM image of the single-crystalline 2D GaN.

(H) A low-magnification TEM image of single-crystalline 2D GaN. Images reproduced F-H with permission from (Chen et al., 2018). Copyright 2018 American Chemical Society.

Confined space can also be constructed by designing a stratified structure. In 2018, Chen et al. reported the successful growth of 2D GaN single crystals by a surface-confined nitridation reaction (SCNR) via a CVD method (Chen et al., 2018). Different from the confined space constructed between graphene and substrate, they designed a surface tension-induced stratified Ga/Ga-W structure. Owing to the smaller surface tension of liquid Ga, Ga atoms occupied the outmost surface area and the subsurface is occupied by Ga-W solid solution, formed Ga/Ga-W structure. In this case, reactive nitrogen atoms decomposed from urea reacted with the surface Ga atoms and formed 2D GaN, as illustrated in Figure 3F. As the nitridation ability of W atoms is stronger than Ga atoms, the vertical growth of GaN was limited. Hence, the growth of 2D GaN was confined on the surface of the Ga/Ga—W structure. The atomic force microscopy (AFM) revealed that the 2D GaN single crystal exhibited a thickness of 4.1 nm (Figure 3G). The high-resolution transmission electron microscopy image further confirmed its ultrathin hexagon morphology (Figure 3H). The difference in nitridation ability provides a new degree of freedom in constructing a confined space.

In summary, the confined environment can be constructed by several strategies such as physical constraint, template-assisted confinement, and stratified structure design. Notably, the designing of stratified structure provides a new perspective on constructing confined spaces. Different types of capping layers significantly affect the growth process in the space confinement strategy. 2D vdW materials used as the capping layer can provide a flat and less reactive surface for the synthesis of ultrathin III-V semiconductors. 3D

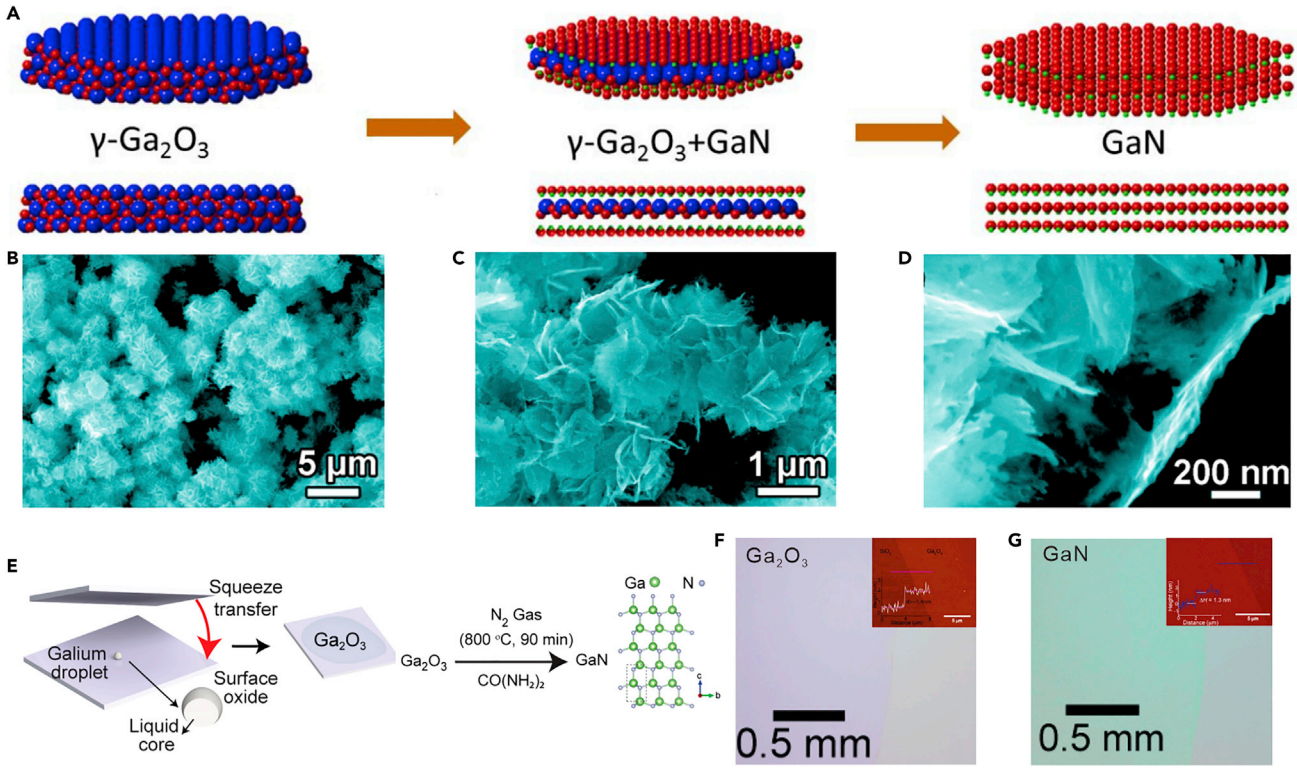

Figure 4. Atomic substitution growth of III-V semiconductors

(A) Schematic diagram of the atomic substitution to formation 2D GaN crystal from Ga_2O_3 nanosheets.

(B–D) TEM images of 2D GaN with different magnifications. Images A-D reproduced with permission from (Liu et al., 2017). Copyright 2017 American Chemical Society.

(E) Schematic diagram of the formation of 2D GaN crystal by nitriding the Ga_2O_3 film.

(F) An optical image of exfoliated Ga_2O_3 film (Inset is AFM of Ga_2O_3 film).

(G) An optical image of 2D GaN (Inset is AFM of 2D GaN). Images E-G reproduced with permission from (Syed et al., 2019). Copyright 2019 American Chemical Society.

capping layer with dangling bonds on the surface will affect the formation of target materials because the dangling bonds may combine or react with active species decomposed from precursors (Suzuki et al., 2021). Precursors are decomposed into reactive species and delivered to the region between capping layer and substrate and form ultrathin III-V semiconductors. Owing to the limit of growing space, the confined growth of 2D non-layered semiconductors can be realized.

Atomic substitution

The atomic substitution strategy always applies accessible 2D materials to derive atomic substitution and conversion, which is effective in the synthesis of 2D non-layered materials currently. Ordinarily, the accessible 2D layered materials obtained by different methods are served as precursors, which can modulate the size and thickness of 2D non-layered materials. This approach gets rid of the shackles of the isotropic growth mode of non-layered materials. Non-layered 2D transition metal nitrides (TMNs) and cadmium sulfide (CdS) were prepared successfully by this strategy (Cao et al., 2020; Zhao et al., 2021). Liu et al. achieved the preparation of ultrathin GaN with mesoporous morphology by this method (Liu et al., 2017). A metastable γ-Ga_2O_3 layer with the smooth surface, crystalline nature, and a thickness of 5–10 nm prepared by a modified hydrothermal method were applied as the precursor. Then, γ-Ga_2O_3 was nitrogenized by NH_3 resulting in a direct structural transformation from γ-Ga_2O_3 phase to hexagonal GaN phase (Figure 4A). The SEM images indicated that the morphology, layer framework, and dispersion of GaN nanosheets remained well (Figures 4B–4D). Here, γ-Ga_2O_3 plays an extremely important role in the structural transformation process. Its unstable structure and the very close lattice constants between (220) crystal plane of cubic structure and the (100) plane of hexagonal GaN enable it easy to undergo structural

transformation. However, the obtained GaN exhibits an inapparent quantum confinement effect owing to the existence of lattice defects (Chen et al., 2019).

Following similar principles, GaS and GaSe are employed as precursors which can be dissociated easily from their bulk counterparts. Simultaneously, GaS and GaSe are easy to be nitrogenized, which have been used to prepare GaN nanowalls (Gautam et al., 2005). Enlightened by this, Sreedhara et al. obtained a few layers of GaS and GaSe by the micro-mechanical exfoliation with scope tape (Sreedhara et al., 2014). Subsequently, GaN can be obtained by heating few-layer GaS or GaSe nanosheets in a tubular furnace, which exhibits high crystallinity and a larger size with hexagonal symmetry.

Liquid metal squeeze-printing oxidation technique was exploited by Syed et al. to obtain centimeter-size Ga_2O_3 film as the precursors to synthesize GaN film (Syed et al., 2019). The method employed the principle that the liquid metal Ga is easy to get oxidized in air and the as-obtained Ga_2O_3 exhibits weak adhesion on the parent Ga metal. As seen in the process shown in Figure 4E, liquid metal was squeezed by two SiO_2/Si wafers with an atomic level flat surface which has van der Waals interaction with Ga_2O_3. The liquid metal Ga was cleaned by the mechanical ethanol washing method. A large and continuous ultrathin Ga_2O_3 film with a transverse dimension of more than a few centimeters and a thickness of 1.4 nm (Insert map of Figure 4F) was obtained as shown in Figure 4F. After that, GaN was obtained by a nitridation process with urea. The scale of GaN obtained by this approach not only reaches the centimeter level (Figure 4G) but also possesses a thickness of only 1.3 nm (Insert map of Figure 4G). Moreover, the wafer-scale and ultrathin 2D InN were also obtained, which illustrated that the method has certain universality.

The target product can be obtained by the atomic substitution strategy from the precursors that are relatively more accessible, which establishes the transition of different 2D crystals, and realizes the preparation of large-scale 2D non-layered materials at the same time.

Adhesion energy regulation

Inherent covalent bondings in non-layered III-V crystals hinder- their layer-by-layer growth mode. It is reported that high adhesion energy between the crystal and substrate will lead to a layer-by-layer growth mode, which provides a feasible path for the synthesis of ultrathin III-V semiconductors (Dick, 2008; Mutaftschiev, 1989). Inspired by this, Chen et al. constructed an $AuIn_2$ alloy substrate with enhanced adhesion energy to promote the layered growth of ultrathin III-V semiconductors (Figure 5A) (Chen et al., 2020). The growth process performed on pure III-group metals suggested that only island growth mode was energetically preferred, which leads to the bulk counterparts finally (Figure 5B). The mechanism was demonstrated convincingly by theoretical calculation, adhesion energy of the InP layer on the $AuIn_2$ alloy is about 1.51 eV $(InP)^{-1}$, which is larger than that on InP (1.08 eV $(InP)^{-1}$) and pure In metal (0.88 eV $(InP)^{-1}$), as shown in Figure 5C. Therefore, $AuIn_2$ was a favorable substrate for the layer-by-layer growth of InP semiconductor. AFM characterization results indicated that the thickness of InP on $AuIn_2$ substrate was only 6.3 nm, which was 600 nm on pure In substrate (Figures 5D and 5E). The corresponding energy-dispersive X-ray spectroscopy (EDS) mapping images and selected area electron diffraction (SAED) pattern in Figures 5F–5H confirmed the samples obtained by substrate adhesion energy regulation are not only uniform but also possess an excellent crystallinity. Further atomic structure analysis by high-angle annular dark-field scanning transmission electron microscope (HAADF-STEM) revealed that the ordered atomic sequences of In and P are consistent with the (111) plane structure (Figure 5I).

A series of III-V semiconductors including GaN, InSb, GaSb, and GaP were prepared by this strategy and the quantum confinement effect was discovered as well. The excellent growth results and universality of this strategy offer a new route for the synthesis of ultrathin III-V semiconductors.

Epitaxial growth

Epitaxial growth strategy is the art of growing single-crystalline films on a crystallographically oriented wafer and is widely used in the growth of ultrathin III-V semiconductors for modern solid-state electronic and photonic devices (Feng et al., 2019; Kim et al., 2017; Kum et al., 2019; Ren et al., 2021). The substrate has a significant effect on the epitaxial growth process such as deposition rate and surface topography (Tung, 1965). Pan et al. reported the successful growth of high-quality single-crystalline 2D InSb nanosheets on Si (111) substrate via molecular beam epitaxy (MBE) (Pan et al., 2016). As illustrated in Figure 6A, Ag was

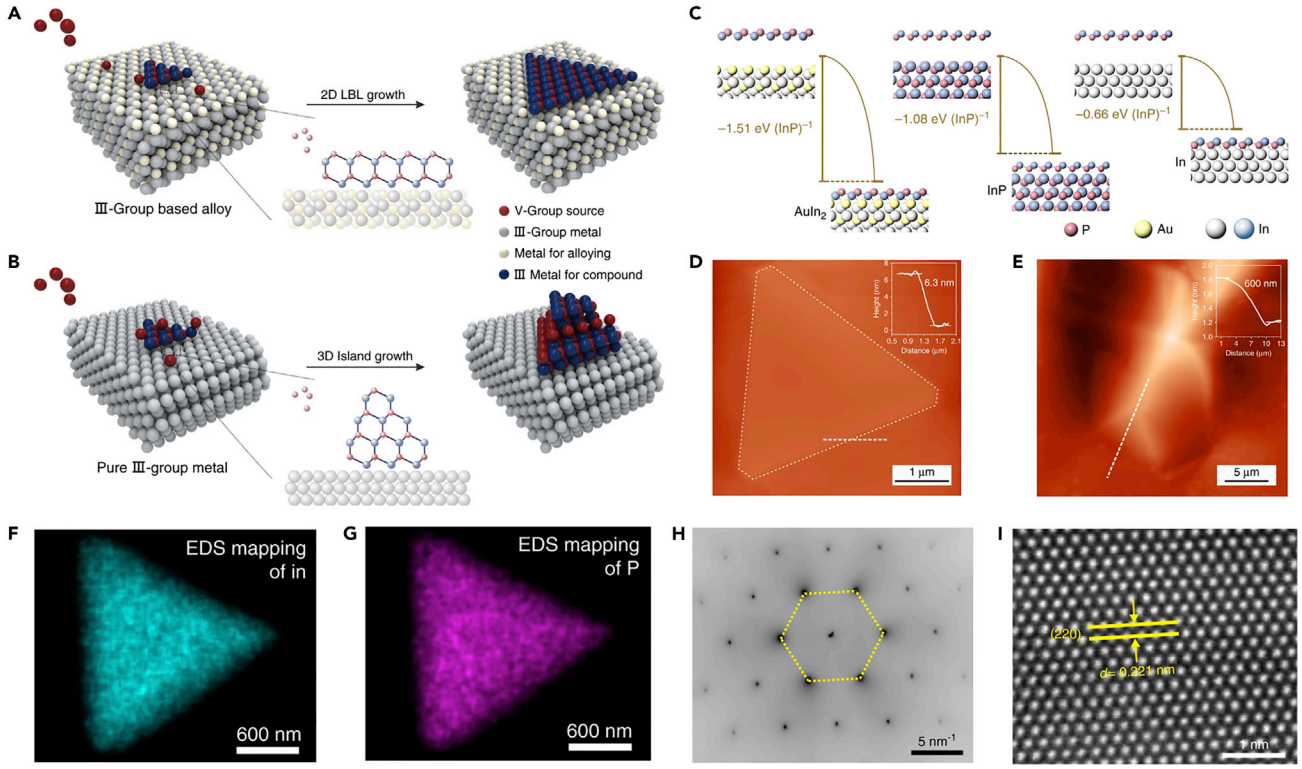

Figure 5. Adhesion energy regulation growth of III-V semiconductors

(A) The mechanism of the layer-by-layer growth mode on alloy substrate of ultra-thin III-V single crystals.

(B) The mechanism of the island growth mode on the pure metal substrate of bulk III-V single crystals.

(C) The adhesion energies between InP and surfaces of $AuIn_2$, InP, and In substrates.

(D) AFM image of ultra-thin III-V single crystals.

(E) AFM image of bulk III-V single crystals.

(F) The EDS mapping of In element in ultra-thin InP single crystals.

(G) The EDS mapping of P element in ultra-thin InP single crystals.

(H) The SAED pattern- of ultra-thin InP single crystal.

(I) The HAADF-STEM image of InP single crystal obtained along the [111] direction. Images A-H reproduced with permission from (Chen et al., 2020). Copyright 2020 Springer Nature.

firstly deposited on the Si (111) substrate as the catalyst in the MBE chamber. The As/In beam equivalent pressure (BEP) ratio was precisely controlled to grow InAs nanowire. Then the As/In source was switched to Sb/In source and InSb was grown on free-standing InAs nanowire stems. HAADF-STEM (Figure 6B) and EDS line profiles further revealed showed that the InAs/InSb heterostructure started as InAs and then transformed to InSb. By tuning the Sb/In BEP ratio, the growth of 2D InSb nanosheets could be realized. Furthermore, the lateral size of InSb nanosheets can be modulated by controlling the growth time, as shown in Figure 6C. With growth time increasing, the size of InSb nanosheets could be micrometers, while their thickness is still kept. The growth of the InSb nanosheets is believed to combine the vapor-liquid-solid growth mode in the vertical direction and the vapor-solid growth mode in the lateral direction.

2D InSb nanostructures can also be epitaxially grown without introducing any foreign template. Gazibegovic et al. realized the epitaxial growth of InSb nanoflakes by using InSb as a substrate (Gazibegovic et al., 2019). The InSb (111) substrate was lithographically patterned by varying the diameter of gold catalyst droplets and pitches. By precisely tuning the droplet size and pitch, the growth of InSb nanoflakes or nanowires could be realized. Figure 6D showed that InSb nanoflakes fraction increased evidently with the increase of total In and Sb precursor flow. The relationship between pitches and InSb nanoflakes fraction for varying total flow was further demonstrated in Figure 6E. It was clear that InSb nanoflakes fraction increased with the increase of pitches and total flow.

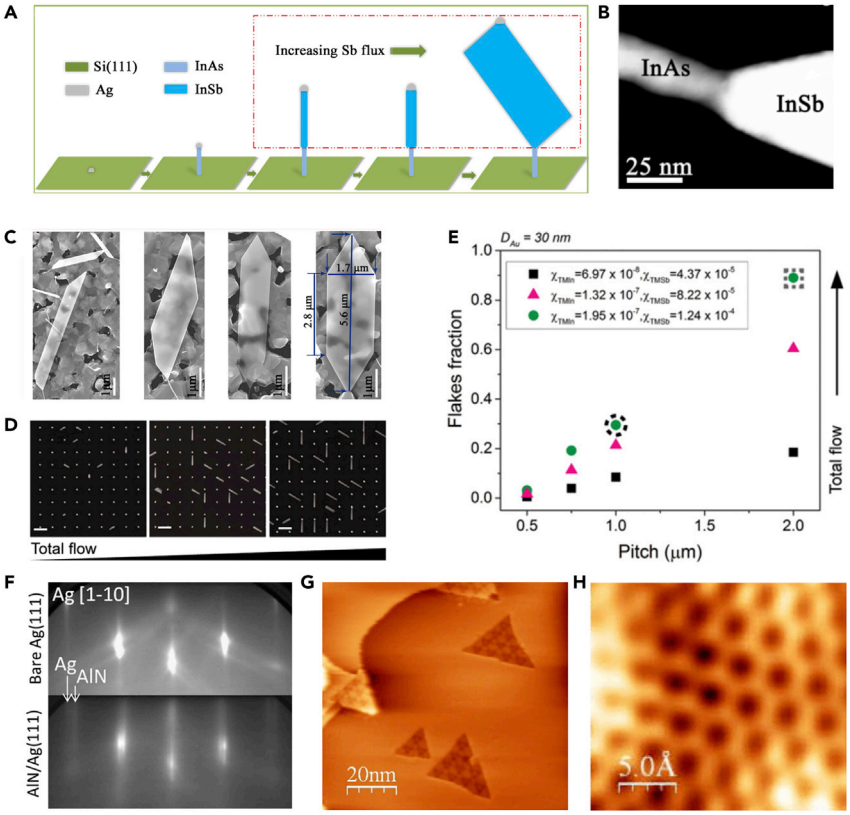

Figure 6. Epitaxial growth of III-V semiconductors

(A) Schematic of the growth process of InSb nanosheets.

(B) HAADF-STEM image of the InAs/InSb interface area.

(C) SEM images of InSb nanosheets with growth time increasing. Images A-C reproduced with permission from (Pan et al., 2016). Copyright 2016 American Chemical Society.

(D) The formation of InSb nanoflakes with the increasing total flow (scale bar: 1 μm).

(E) The relationship between InSb nanoflakes fraction and pitch and total gas flow. Images D and E reproduced with permission from (Gazibegovic et al., 2019). Copyright 2019 American Chemical Society.

(F) RHEED patterns of bare Ag (111) and AlN/Ag (111) structures.

(G) STM topography of 2D AlN on Ag (111).

(H) Atomic resolution STM topography of 2D AlN. Images F-H reproduced with permission from (Tsipas et al., 2013). Copyright 2013 AIP Publishing.

Ag can be a suitable substrate for the epitaxial growth of 2D AlN for its small lattice mismatch. 2D AlN nanosheets were prepared on single-crystal Ag (111) substrate via plasma-assisted MBE (Tsipas et al., 2013). As shown in Figure 6F, the reflection high-energy electron diffraction (RHEED) pattern of Ag along [1–10] indicated that Ag (111) substrate had a flat surface, the extra streak in the RHEED pattern confirmed the epitaxial growth of flat AlN. The scanning tunneling microscopy (STM) topography in Figure 6G showed the formation of well-defined 2D AlN islands. Furthermore, high-resolution STM topography in Figure 6H clearly displayed the honeycomb-like structure of 2D AlN nanosheets.

CONCLUSION AND OUTLOOK

Ascribed to the intrinsic structure and excellent characteristics, ultrathin III-V semiconductors have attracted more and more interest from researchers, especially in the synthesis strategy that is important in the development of ultrathin III-V semiconductors. For the space confinement strategy, it realizes the synthesis of ultrathin III-V semiconductors by constructing a space to restrain the vertical growth. It is a general method to synthesize ultrathin III-V semiconductors currently. However, this method is difficult to accurately control the thickness of ultrathin III-V semiconductors because it's challenging to control the vertical

size of the confined space. The atom substitution strategy can effectively control the thickness of ultrathin III-V semiconductors by controlling the thickness of precursor compounds. However, the choice of precursor compounds is limited. The adhesion energy regulation is to modify the substrate so that the interaction between the substrate and III-V semiconductors is suitable. Obviously, the strict requirements of substrate limit the generalization of this strategy. The epitaxial growth of ultrathin III-V semiconductors is mainly affected by the interaction between the deposited materials and substrate, so it's significant to find a well-matched substrate for the epitaxial growth of ultrathin III-V semiconductors.

In short, the reported methods currently are efficient in the preparation of ultrathin III-V semiconductors, which will lay the foundation for a thorough study and understanding of the properties and applications of them. However, from the outlook of synthesis in ultrathin III-V semiconductors, more efforts should be devoted to the following challenges: (1) Growth of wafer-size single-crystalline ultrathin III-V semiconductors: wafer-scale preparation is essential in the practical application of materials. Therefore, the further development of ultrathin III-V semiconductors must be based on the realization of wafer-size synthesis. The suitable substrates may be helpful for the growth of wafer-size ultrathin III-V semiconductors. Metal substrates or van der Waals substrates are considered to be preferable substrates. The weak dangling bonds of them will enhance the migration of precursor atoms instead of bounding them, which is advantageous for wafer-scale growth (Ben et al., 2021; Yu et al., 2020). Besides, designing the substrate toward effectively regulating the nucleation energy of crystal and realizing the directional growth has been generally applied in the wafer-size growth of 2D layered materials recently (Bubnova, 2021). We can expect that it may also be feasible in the wafer-size growth of ultrathin III-V semiconductors. (2) Preparation of monolayer III-V semiconductors: the thickness reduction of monolayer III-V semiconductors leads to many new properties which have been predicted, but it's difficult to make a thorough inquiry. A bright perspective will be brought by the synthesis of monolayer III-V semiconductors (Zhuang et al., 2013). Recently, salt-assisted CVD growth has been developed to grow ultrathin non-layered materials. The addition of salt leads to the decrease of the melting point of the precursor, the formation of highly active intermediates, the reduction of reaction activation energy, and the increase of reaction rate. Based on these advantages, combining salt with space confinement or suitable substrate designing may enable the synthesis of monolayer III-V semiconductors in the future (Han et al., 2019). (3) Preparation of heterojunction based on III-V semiconductors: theoretical studies suggest that the heterojunctions based on III-V semiconductors will show stronger properties than intrinsic materials in some aspects. For example, the photocatalytic water splitting property of 2D GaN/MoS_2 heterostructure is better than MoS_2 (Liao et al., 2014). Owing to the strong covalent bondings that exist in III-V semiconductors, lattice mismatch will influence the fabrication process of other 2D materials. Therefore, mechanical transfer may be the most practicable method in the synthesis of ultrathin III-V semiconductor heterojunctions. (4) Preparation of hybrid ultrathin III-V semiconductors with dopants: chemical doping is an ordinary modification method that can bring unique properties and functions (Dai et al., 2011). The preparation of hybrid ultrathin III-V semiconductors by doping of different dopants may lead to new phenomena, such as magnetic and half-metal characteristics (Zhao et al., 2016). Many methods are employed to prepare doped compounds. For III-V semiconductors, selecting a suitable precursor for doping is necessary, which is volatile and has well-matched atomic radius with III-V semiconductors. (5) Preparation of ultrathin III-V semiconductors exposed with different planes: the results of theoretical research suggested that ultrathin III-V semiconductors in different planes will show different properties. Four typical planes exist in GaN films: polar c-plane, semipolar r-plane, non-polar a-plane, and m-plane. It is necessary to study the differences between them (Cai et al., 2021). An appropriate crystal facet controller has been selected to effectively control the exposed crystal facet of the 2D materials, which is useful and enlightening in preparing the III-V semiconductors with different facets (Li et al., 2021). (6) Preparation of twist-angle ultrathin III-V semiconductors: the growing research of twisted bilayer graphene in recent years reveals many unique electronic properties, which brings inspiration for the study of other 2D materials with twist angles. Ultrathin III-V semiconductors with twist angles may display unique properties for their exotic structure which is different from layered materials. Stacking may achieve the synthesis of twist-angle ultrathin III-V semiconductors, which is a useful method in twist-angle graphene (Liao et al., 2015).

In summary, it is indisputable that the excellent properties will bring infinite possibilities to ultrathin III-V semiconductors, and these possibilities will be realized eventually only if the synthesis strategies tend to be mature in the future.

ACKNOWLEDGMENTS

The research was supported by the National Natural Science Foundation of China (grants 22025303 and 21905210) and the Sino-German Center for Research Promotion (grant no. 1400).

AUTHOR CONTRIBUTIONS

L.F., and M.Q.Z. conceived the idea and designed the frame. L.F. and M.Q.Z. supervised the project. F.Y.L. and H.L.W. wrote the first draft of the manuscript. All authors commented, edited, and revised the final manuscript.

CONFLICTS OF INTEREST

The authors declare no competing interests.

REFERENCES

Al Balushi, Z.Y., Wang, K., Ghosh, R.K., Vilá, R.A., Eichfeld, S.M., Caldwell, J.D., Qin, X., Lin, Y.-C., DeSario, P.A., Stone, G., et al. (2016). Two-dimensional gallium nitride realized via graphene encapsulation. Nat. Mater. *15*, 1166–1171. https://doi.org/10.1038/nmat4742.

Ambacher, O., Smart, J., Shealy, J.R., Weimann, N.G., Chu, K., Murphy, M., Schaff, W.J., Eastman, L.F., Dimitrov, R., Wittmer, L., et al. (1999). Two-dimensional electron gases induced by spontaneous and piezoelectric polarization charges in N- and Ga-face AlGaN/GaN heterostructures. J. Appl. Phys. *85*, 3222–3323. https://doi.org/10.1063/1.369664.

Ben, J., Liu, X., Wang, C., Zhang, Y., Shi, Z., Jia, Y., Zhang, S., Zhang, H., Yu, W., Li, D., and Sun, X. (2021). 2D III-Nitride materials: properties, growth, and applications. Adv. Mater. *33*, e2006761. https://doi.org/10.1002/adma.202006761.

Blonsky, M.N., Zhuang, H.L., Singh, A.K., and Hennig, R.G. (2015). Ab Initio prediction of piezoelectricity in two-dimensional materials. ACS Nano *9*, 9885–9891. https://doi.org/10.1021/acsnano.5b03394.

Brus, L.E. (1984). Electron-electron and electron-hole interactions in small semiconductor crystallites: the size dependence of the lowest excited electronic state. J. Chem. Phys. *80*, 4403–4409. https://doi.org/10.1063/1.447218.

Bubnova, O. (2021). 2D materials grow large. Nat. Nanotech. *16*, 1179. https://doi.org/10.1038/s41565-021-01024-w.

Cai, X., Ma, Y., Ma, J., Xu, D., and Luo, X. (2021). Structure and electronic bandgap tunability of m-plane GaN multilayers. Phys. Chem. Chem. Phys. *23*, 5431–5437. https://doi.org/10.1039/D0CP06093C.

Cao, J., Li, T., Gao, H., Lin, Y., Wang, X., Wang, H., Palacios, T., and Ling, X. (2020). Realization of 2D crystalline metal nitrides via selective atomic substitution. Sci. Adv. *6*, eaax8784. https://doi.org/10.1126/sciadv.aax8784.

Chaudhuri, R., Bader Samuel, J., Chen, Z., Muller David, A., Xing Huili, G., and Jena, D. (2019). A polarization-induced 2D hole gas in undoped gallium nitride quantum wells. Science *365*, 1454–1457. https://doi.org/10.1126/science.aau8623.

Chen, K., Kapadia, R., Harker, A., Desai, S., Seuk Kang, J., Chuang, S., Tosun, M., Sutter-Fella, C.M., Tsang, M., Zeng, Y., et al. (2016). Direct growth of single-crystalline III-V semiconductors on amorphous substrates. Nat. Commun. *7*, 10502. https://doi.org/10.1038/ncomms10502.

Chen, Y., Liu, J., Liu, K., Si, J., Ding, Y., Li, L., Lv, T., Liu, J., and Fu, L. (2019). GaN in different dimensionalities: properties, synthesis, and applications. Mater. Sci. Eng. R. Rep. *138*, 60–84. https://doi.org/10.1016/j.mser.2019.04.001.

Chen, Y., Liu, J., Zeng, M., Lu, F., Lv, T., Chang, Y., Lan, H., Wei, B., Sun, R., Gao, J., et al. (2020). Universal growth of ultra-thin III-V semiconductor single crystals. Nat. Commun. *11*, 3979. https://doi.org/10.1038/s41467-020-17693-5.

Chen, Y., Liu, K., Liu, J., Lv, T., Wei, B., Zhang, T., Zeng, M., Wang, Z., and Fu, L. (2018). Growth of 2D GaN single crystals on liquid metals. J. Am. Chem. Soc. *140*, 16392–16395. https://doi.org/10.1021/jacs.8b08351.

Cipriano, L.A., Di Liberto, G., Tosoni, S., and Pacchioni, G. (2020). Quantum confinement in group III-V semiconductor 2D nanostructures. Nanoscale *12*, 17494–17501. https://doi.org/10.1039/D0NR03577G.

Cipriano, L.A., Di Liberto, G., Tosoni, S., and Pacchioni, G. (2021). Structure and band alignment of InP photocatalysts passivated by TiO_2 thin films. J. Phys. Chem. C *125*, 11620–11627. https://doi.org/10.1021/acs.jpcc.1c01666.

Dai, Z., Nurbawono, A., Zhang, A., Zhou, M., Feng, Y.P., Ho, G.W., and Zhang, C. (2011). C-doped ZnO nanowires: electronic structures, magnetic properties, and a possible spintronic device. J. Chem. Phys. *134*, 104706. https://doi.org/10.1063/1.3562375.

del Alamo, J.A. (2011). Nanometre-scale electronics with III-V compound semiconductors. Nature *479*, 317–323. https://doi.org/10.1038/nature10677.

Dick, K.A. (2008). A review of nanowire growth promoted by alloys and non-alloying elements with emphasis on Au-assisted III-V nanowires. Prog. Cryst. Growth Charact. Mater. *54*, 138–173. https://doi.org/10.1016/j.pcrysgrow.2008.09.001.

Dou, Y., Zhang, L., Xu, X., Sun, Z., Liao, T., and Dou, S.X. (2017). Atomically thin non-layered nanomaterials for energy storage and conversion. Chem. Soc. Rev. *46*, 7338–7373. https://doi.org/10.1039/C7CS00418D.

Feng, J., Sun, X., Wu, C., Peng, L., Lin, C., Hu, S., Yang, J., and Xie, Y. (2011). Metallic few-layered VS_2 ultrathin nanosheets: high two-dimensional conductivity for in-plane supercapacitors. J. Am. Chem. Soc. *133*, 17832–17838. https://doi.org/10.1021/ja207176c.

Feng, Y., Yang, X., Zhang, Z., Kang, D., Zhang, J., Liu, K., Li, X., Shen, J., Liu, F., Wang, T., et al. (2019). Epitaxy of single-crystalline GaN film on CMOS-compatible Si(100) substrate buffered by graphene. Adv. Funct. Mater. *29*, 1905056. https://doi.org/10.1002/adfm.201905056.

Gautam, U.K., Vivekchand, S.R.C., Govindaraj, A., and Rao, C.N.R. (2005). GaS and GaSe nanowalls and their transformation to Ga_2O_3 and GaN nanowalls. Chem. Commun. *31*, 3995–3997. https://doi.org/10.1039/B506676J.

Gazibegovic, S., Badawy, G., Buckers, T.L.J., Leubner, P., Shen, J., de Vries, F.K., Koelling, S., Kouwenhoven, L.P., Verheijen, M.A., and Bakkers, E.P.A.M. (2019). Bottom-up grown 2D InSb nanostructures. Adv. Mater. *31*, 1808181. https://doi.org/10.1002/adma.201808181.

Han, W., Liu, K., Yang, S., Wang, F., Su, J., Jin, B., Li, H., and Zhai, T. (2019). Salt-assisted chemical vapor deposition of two-dimensional materials. Sci. China Chem. *62*, 1300–1311. https://doi.org/10.1007/s11426-019-9525-y.

Hu, S., Shaner Matthew, R., Beardslee Joseph, A., Lichterman, M., Brunschwig Bruce, S., and Lewis Nathan, S. (2014). Amorphous TiO_2 coatings stabilize Si, GaAs, and GaP photoanodes for efficient water oxidation. Science *344*, 1005–1009. https://doi.org/10.1126/science.1251428.

Kim, Y., Cruz, S.S., Lee, K., Alawode, B.O., Choi, C., Song, Y., Johnson, J.M., Heidelberger, C., Kong, W., Choi, S., et al. (2017). Remote epitaxy through graphene enables two-dimensional material-based layer transfer. Nature *544*, 340–343. https://doi.org/10.1038/nature22053.

Kobayashi, Y., Kumakura, K., Akasaka, T., and Makimoto, T. (2012). Layered boron nitride as a release layer for mechanical transfer of GaN-based devices. Nature *484*, 223–227. https://doi.org/10.1038/nature10970.

Kolobov, A.V., Fons, P., Tominaga, J., Hyot, B., and André, B. (2016). Instability and spontaneous reconstruction of few-monolayer thick GaN graphitic structures. Nano Lett. *16*, 4849–4856. https://doi.org/10.1021/acs.nanolett.6b01225.

Kuech, T.F. (2016). III-V compound semiconductors: growth and structures. Prog. Cryst. Growth Charact. Mater. *62*, 352–370. https://doi.org/10.1016/j.pcrysgrow.2016.04.019.

Kum, H., Lee, D., Kong, W., Kim, H., Park, Y., Kim, Y., Baek, Y., Bae, S.-H., Lee, K., and Kim, J. (2019). Epitaxial growth and layer-transfer techniques for heterogeneous integration of materials for electronic and photonic devices. Nat. Electron. *2*, 439–450. https://doi.org/10.1038/s41928-019-0314-2.

Kumar, N., Najmaei, S., Cui, Q., Ceballos, F., Ajayan, P.M., Lou, J., and Zhao, H. (2013). Second harmonic microscopy of monolayer MoS_2. Phys. Rev. B *87*, 161403. https://doi.org/10.1103/PhysRevB.87.161403.

Li, S., Lin, Y.-C., Zhao, W., Wu, J., Wang, Z., Hu, Z., Shen, Y., Tang, D.-M., Wang, J., Zhang, Q., et al. (2018). Vapour-liquid-solid growth of monolayer MoS_2 nanoribbons. Nat. Mater. *17*, 535–542. https://doi.org/10.1038/s41563-018-0055-z.

Li, L., Lu, F., Xiong, W., Ding, Y., Lu, Y., Xiao, Y., Tong, X., Wang, Y., Jia, S., Wang, J., et al. (2021). General synthesis of 2D rare-earth oxides single crystals with tailorable facet. Natl. Sci. Rev. *8*, nwab153. https://doi.org/10.1093/nsr/nwab153.

Liang, D., Quhe, R., Chen, Y., Wu, L., Wang, Q., Guan, P., Wang, S., and Lu, P. (2017). Electronic and excitonic properties of two-dimensional and bulk InN crystals. RSC Adv. *7*, 42455–42461. https://doi.org/10.1039/C7RA07640A.

Liao, J., Sa, B., Zhou, J., Ahuja, R., and Sun, Z. (2014). Design of high-efficiency visible-light photocatalysts for water-splitting: MoS_2/AlN(GaN) heterostructures. J. Phys. Chem. C *118*, 17594–17599. https://doi.org/10.1021/jp5038014.

Liao, L., Wang, H., Peng, H., Yin, J., Koh, A.L., Chen, Y., Xie, Q., Peng, H., and Liu, Z. (2015). Van hove singularity enhanced photochemical reactivity of twisted bilayer graphene. Nano Lett. *15*, 5585–5589. https://doi.org/10.1021/acs.nanolett.5b02240.

Liu, B., Yang, W., Li, J., Zhang, X., Niu, P., and Jiang, X. (2017). Template approach to crystalline GaN nanosheets. Nano Lett. *17*, 3195–3201. https://doi.org/10.1021/acs.nanolett.7b00754.

Liu, H., Neal, A.T., Zhu, Z., Luo, Z., Xu, X., Tománek, D., and Ye, P.D. (2014). Phosphorene: an unexplored 2D semiconductor with a high hole mobility. ACS Nano *8*, 4033–4041. https://doi.org/10.1021/nn501226z.

Long, M.-Q., Tang, L., Wang, D., Wang, L., and Shuai, Z. (2009). Theoretical predictions of size-dependent carrier mobility and polarity in graphene. J. Am. Chem. Soc. *131*, 17728–17729. https://doi.org/10.1021/ja907528a.

Mishra, A., Mehta, A., Basu, S., Shetti, N.P., Reddy, K.R., and Aminabhavi, T.M. (2019). Graphitic carbon nitride (g-C_3N_4) -based metal-free photocatalysts for water splitting: a review. Carbon *149*, 693–721. https://doi.org/10.1016/j.carbon.2019.04.104.

Mutaftschiev, B. (1989). Wetting and displacement of three-dimensional and two-dimensional layers on a foreign substrate. Phys. Rev. B *40*, 779–782. https://doi.org/10.1103/PhysRevB.40.779.

Novoselov, K.S., Geim, A.K., Morozov, S.V., Jiang, D., Zhang, Y., Dubonos, S.V., Grigorieva, I.V., and Firsov, A.A. (2004). Electric field effect in atomically thin carbon films. Science *306*, 666–669. https://doi.org/10.1126/science.1102896.

Pan, D., Fan, D.X., Kang, N., Zhi, J.H., Yu, X.Z., Xu, H.Q., and Zhao, J.H. (2016). Free-standing two-dimensional single-crystalline InSb nanosheets. Nano Lett. *16*, 834–841. https://doi.org/10.1021/acs.nanolett.5b04845.

Pécz, B., Nicotra, G., Giannazzo, F., Yakimova, R., Koos, A., and Kakanakova-Georgieva, A. (2021). Indium nitride at the 2D limit. Adv. Mater. *33*, 2006660. https://doi.org/10.1002/adma.202006660.

Qin, Z., Qin, G., Zuo, X., Xiong, Z., and Hu, M. (2017). Orbitally driven low thermal conductivity of monolayer gallium nitride (GaN) with planar honeycomb structure: a comparative study. Nanoscale *9*, 4295–4309. https://doi.org/10.1039/C7NR01271C.

Ren, F., Liu, B., Chen, Z., Yin, Y., Sun, J., Zhang, S., Jiang, B., Liu, B., Liu, Z., Wang, J., et al. (2021). Van der Waals epitaxy of nearly single-crystalline nitride films on amorphous graphene-glass wafer. Sci. Adv. *7*, eabf5011. https://doi.org/10.1126/sciadv.abf5011.

Riedl, C., Coletti, C., Iwasaki, T., Zakharov, A.A., and Starke, U. (2009). Quasi-free-standing epitaxial graphene on SiC obtained by hydrogen intercalation. Phys. Rev. Lett. *103*, 246804. https://doi.org/10.1103/PhysRevLett.103.246804.

Şahin, H., Cahangirov, S., Topsakal, M., Bekaroglu, E., Akturk, E., Senger, R.T., and Ciraci, S. (2009). Monolayer honeycomb structures of group-IV elements and III-V binary compounds: first-principles calculations. Phys. Rev. B *80*, 155453. https://doi.org/10.1103/PhysRevB.80.155453.

Sanders, N., Bayerl, D., Shi, G., Mengle, K.A., and Kioupakis, E. (2017). Electronic and optical properties of two-dimensional GaN from first-principles. Nano Lett. *17*, 7345–7349. https://doi.org/10.1021/acs.nanolett.7b03003.

Schmidt, H., Wang, S., Chu, L., Toh, M., Kumar, R., Zhao, W., Castro Neto, A.H., Martin, J., Adam, S., Özyilmaz, B., and Eda, G. (2014). Transport properties of monolayer MoS_2 grown by chemical vapor deposition. Nano Lett. *14*, 1909–1913. https://doi.org/10.1021/nl4046922.

Sreedhara, M.B., Vasu, K., and Rao, C.N.R. (2014). Synthesis and characterization of few-layer nanosheets of GaN and other metal nitrides. Z. Anorg. Allg. Chem. *640*, 27374–27382. https://doi.org/10.1002/zaac.201400386.

Suzuki, S., Iwasaki, T., De Silva, K.K.H., Suehara, S., Watanabe, K., Taniguchi, T., Moriyama, S., Yoshimura, M., Aizawa, T., and Nakayama, T. (2021). Direct growth of germanene at interfaces between van der Waals materials and Ag(111). Adv. Funct. Mater. *31*, 2007038. https://doi.org/10.1002/adfm.202007038.

Syed, N., Zavabeti, A., Messalea, K.A., Della Gaspera, E., Elbourne, A., Jannat, A., Mohiuddin, M., Zhang, B.Y., Zheng, G., Wang, L., et al. (2019). Wafer-sized ultrathin gallium and indium nitride nanosheets through the ammonolysis of liquid metal derived oxides. J. Am. Chem. Soc. *141*, 104–108. https://doi.org/10.1021/jacs.8b11483.

Tang, Q., and Jiang, D.-C. (2016). Mechanism of hydrogen evolution reaction on 1T-MoS_2 from first principles. ACS Catal. *6*, 4953–4961. https://doi.org/10.1021/acscatal.6b01211.

Tsipas, P., Kassavetis, S., Tsoutsou, D., Xenogiannopoulou, E., Golias, E., Giamini, S.A., Grazianetti, C., Chiappe, D., Molle, A., Fanciulli, M., and Dimoulas, A. (2013). Evidence for graphite-like hexagonal AlN nanosheets epitaxially grown on single crystal Ag(111). Appl. Phys. Lett. *103*, 251605. https://doi.org/10.1063/1.4851239.

Tung, S.K. (1965). The effects of substrate orientation on epitaxial growth. J. Electrochem. Soc. *112*, 436–438. https://doi.org/10.1149/1.2423563.

Van Dao, D., Cipriano, L.A., Di Liberto, G., Nguyen, T.T.D., Ki, S.-W., Son, H., Kim, G.-C., Lee, K.H., Yang, J.-K., Yu, Y.-T., et al. (2021). Plasmonic Au nanoclusters dispersed in nitrogen-doped graphene as a robust photocatalyst for light-to-hydrogen conversion. J. Mater. Chem. A. *9*, 22810–22819. https://doi.org/10.1039/D1TA05445G.

Wallentin, J., Anttu, N., Asoli, D., Huffman, M., Åberg, I., Magnusson Martin, H., Siefer, G., Fuss-Kailuweit, P., Dimroth, F., Witzigmann, B., et al. (2013). InP nanowire array solar cells achieving 13.8% efficiency by exceeding the ray optics limit. Science *339*, 1057–1060. https://doi.org/10.1126/science.1230969.

Wang, B., Wang, D., Ning, J., Zhang, J., and Hao, Y. (2021). Robust magnetic behavior in two-dimensional GaN caused by atomic vacancies. J. Mater. Sci. *56*, 2311–2322. https://doi.org/10.1007/s10853-020-05395-8.

Wang, F., Wang, Z., Shifa, T.A., Wen, Y., Wang, F., Zhan, X., Wang, Q., Xu, K., Huang, Y., Yin, L., et al. (2017a). Two-dimensional non-layered materials: synthesis, properties and applications. Adv. Funct. Mater. *27*, 1603254. https://doi.org/10.1002/adfm.201603254.

Wang, P., Wang, T., Wang, H., Sun, X., Huang, P., Sheng, B., Rong, X., Zheng, X., Chen, Z., Wang, Y., et al. (2019a). Experimental evidence of large bandgap energy in atomically thin AlN. Adv. Funct. Mater. *29*, 1902608. https://doi.org/10.1002/adfm.201902608.

Wang, Q., Yang, F., Zhang, Y., Chen, M., Zhang, X., Lei, S., Li, R., and Hu, W. (2018a). Space-confined strategy toward large-area two-dimensional single crystals of molecular materials. J. Am. Chem. Soc. *140*, 5339–5342. https://doi.org/10.1021/jacs.8b01997.

Wang, T., Chen, S., Pang, H., Xue, H., and Yu, Y. (2017b). MoS_2-based nanocomposites for electrochemical energy storage. Adv. Sci. *4*, 1600289. https://doi.org/10.1002/advs.201600289.

Wang, W., Zheng, Y., Li, X., Li, Y., Zhao, H., Huang, L., Yang, Z., Zhang, X., and Li, G. (2019b). 2D AlN layers sandwiched between graphene and Si

substrates. Adv. Mater. *31*, 1803448. https://doi.org/10.1002/adma.201803448.

Wang, Y., Song, N., Song, X., Zhang, T., Yang, D., and Li, M. (2018b). A first-principles study of gas adsorption on monolayer AlN sheet. Vacuum *147*, 18–23. https://doi.org/10.1016/j.vacuum.2017.10.014.

Yeganeh, M., Kafi, F., and Boochani, A. (2020). Thermoelectric properties of InN graphene-like nanosheet: a first principle study. Superlattice. Microstruct. *138*, 106367. https://doi.org/10.1016/j.spmi.2019.106367.

Yu, J., Wang, L., Hao, Z., Luo, Y., Sun, C., Wang, J., Han, Y., Xiong, B., and Li, H. (2020). Van der Waals epitaxy of III–semiconductors based on 2D materials for flexible applications. Adv. Mater. *32*, 1903407. https://doi.org/10.1002/adma.201903407.

Zeng, G., Qiu, J., Hou, B., Shi, H., Lin, Y., Hettick, M., Javey, A., and Cronin, S.B. (2015). Enhanced photocatalytic reduction of CO_2 to CO through TiO_2 passivation of InP in ionic liquids. Chem. Eur. J. *21*, 13502–13507. https://doi.org/10.1002/chem.201501671.

Zhang, G., Takiguchi, M., Tateno, K., Tawara, T., Notomi, M., and Gotoh, H. (2019). Telecom-band lasing in single InP/InAs heterostructure nanowires at room temperature. Sci. Adv. *5*, eaat8896. https://doi.org/10.1126/sciadv.aat8896.

Zhang, H. (2015). Ultrathin two-dimensional nanomaterials. ACS Nano *9*, 9451–9469. https://doi.org/10.1021/acsnano.5b05040.

Zhao, M., Yang, S., Zhang, K., Zhang, L., Chen, P., Yang, S., Zhao, Y., Ding, X., Zu, X., Li, Y., et al. (2021). A universal atomic substitution conversion strategy towards synthesis of large-size ultrathin non-layered two-dimensional materials. Nano-Micro Lett. *13*, 165. https://doi.org/10.1007/s40820-021-00692-6.

Zhao, Q., Xiong, Z., Qin, Z., Chen, L., Wu, N., and Li, X. (2016). Tuning magnetism of monolayer GaN by vacancy and nonmagnetic chemical doping. J. Phys. Chem. Sol. *91*, 1–6. https://doi.org/10.1016/j.jpcs.2015.12.002.

Zhi, C., Bando, Y., Tang, C., Kuwahara, H., and Golberg, D. (2009). Large-scale fabrication of boron nitride nanosheets and their utilization in polymeric composites with improved thermal and mechanical properties. Adv. Mater. *21*, 2889–2893. https://doi.org/10.1002/adma.200900323.

Zhi, J., Kang, N., Su, F., Fan, D., Li, S., Pan, D., Zhao, S.P., Zhao, J., and Xu, H.Q. (2019). Coexistence of induced superconductivity and quantum Hall states in InSb nanosheets. Phys. Rev. B *99*, 245302. https://doi.org/10.1103/PhysRevB.99.245302.

Zhou, S., Gan, L., Wang, D., Li, H., and Zhai, T. (2018). Space-confined vapor deposition synthesis of two dimensional materials. Nano Res. *11*, 2909–2931. https://doi.org/10.1007/s12274-017-1942-3.

Zhu, Y., Murali, S., Stoller Meryl, D., Ganesh, K.J., Cai, W., Ferreira Paulo, J., Pirkle, A., Wallace Robert, M., Cychosz Katie, A., Thommes, M., et al. (2011). Carbon-based supercapacitors produced by activation of graphene. Science *332*, 1537–1541. https://doi.org/10.1126/science.1200770.

Zhuang, H.L., Singh, A.K., and Hennig, R.G. (2013). Computational discovery of single-layer III-V materials. Phys. Rev. B *87*, 165415. https://doi.org/10.1103/PhysRevB.87.165415.